Task 1. Diffractometry of polycrystalline thin film

1.1. Task

Experiment of polycrystalline thin film diffraction, phase analysis, Rietveld refinement

1.2. Theory

The experiment is performed with monochromatic x-ray beam. Let us assume the polycrystalline grains are small, thus the irradiated volume contains huge number of grains. The diffraction condition is satisfied only for small number of grains

$$2d \sin\theta = n\lambda\,, \tag{1.1}$$

where angle of incidence equals Bragg angle θ, d is inter-planar distance, n diffraction order and λ wavelength of x-ray radiation.

The intensity of particular diffraction peak is given by structure factor, depending of structure of crystallographic unit cell

$$F(\boldsymbol{h}) = \sum_{i=1}^{N} f_i(h) \mathrm{e}^{-\mathrm{i}\boldsymbol{h}\cdot\boldsymbol{r}_i}, \tag{1.2}$$

where summation runs over N atoms in the unit cell, $\boldsymbol{h}$ is diffraction vector, $f_i(h)$ is atomic form factor of i-th atom in the unit cell and $\boldsymbol{r}_i$ its position. Several high symmetry types of unit cells have certain selection rules of forbidden reflection where structure factor equals zero.

For cubic crystals following selection rules for allowed reflections apply:
simple cubic lattice – all reflections are allowed,
face centered cubic – only those are allowed for which Laue indices have same parity,
body centered cubic – allowed diffractions have $h+k+l$ even,
diamond lattice – all Laue indices odd; or all Laue indices are even and their sum is divisible by 4.

1.3. Experimental setup

Angular distribution of diffracted intensity will be measured in Bragg-Brentano setup and grazing-incidence diffraction setup for thin films.

1.3..1 Bragg-Brentano method

The principle of Bragg-Brentano is shown in figure 1.1. Let us assume the x-ray source S is ideal points source and both source and detector D are moving along circle with the goniometer radius k_{BB}. The sample is positioned in the center of the goniometer circle k_{BB}. If the sample was circular with radius kv defined by source S, detector D and goniometer center V, the beam from the point source scattered at any sample point with scattering angle of 2θ would meet at the same detector point D. In reality we use flat samples; the focusing condition is still satisfied as far as the sample is small with respect to the radius of focusing circle.

In reality we will measure with setup shown in figure 1.2. The divergence of the primary beam is limited by a divergence slit. The detection is performed with linear position sensitive detector. We are using copper x-ray tube with dominant Kα1 line with wavelength of 1,540601 Å and Kα2 line 1,544430 Å. Kβ line is suppressed using nickel filter in the scattered beam. Soller slits are used to define the divergence in the direction perpendicular to the diffraction plane.

First we have to align the diffractometer and sample. We cane use automatic macros which align the beam to the center of the goniometer and also sample surface to the center of goniometer. Measurement is the performed for the selected rage of scattering angles, typically 15–120°. Angular step size in the selected setup can be set to $\Delta 2\theta = 0.01°$. Better angular resolution cannot be achieved because of detector pixel size. The date are saved in the text format with column corresponding to 2θ angle and the second column to scattered intensity.

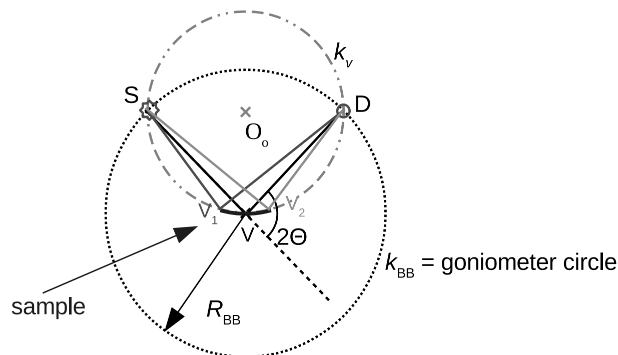

Obrázek 1.1. Principle of Bragg–Brentano setup for powder diffraction. X-ray is originating in a point source S and is detected by a point detector D.

1.4. Evaluation of diffraction peak positions

The lattice parameters can be determined from peak positions only. If the lattice is cubic you can simply determine lattice parameter by following procedure

1. Determine angular positions of diffraction peaks in 2θ. At high angles the profiles are split, why?
2. Sort the positions and try to find corresponding allowed Laue indices $N = h^2 + k^2 + l^2$ for translation type. Well corresponding type should give same lattice parameter given by formula (1.1) for any diffraction order.
3. determine average lattice parameter. Every diffraction line has different uncertainty of lattice parameter determination; higher orders leads to a more precise determination. We suggest to use weighted average

$$\bar{a} = \frac{\sum_{i=1}^{n} w_i a_i}{\sum_{i=1}^{n} w_i}, \tag{1.3}$$

where the weight is inversely proportional to a standard uncertainty of each point σ_i as $w_i = 1/\sigma_i^2$. The standard deviation of weighted average is then

$$\sigma_{\bar{a}}^2 = \frac{1}{(n-1)\sum_{i=1}^{n} w_i} \sum_{i=1}^{n} w_i (a_i - \bar{a})^2, \tag{1.4}$$

where n is number of measured diffraction lines.

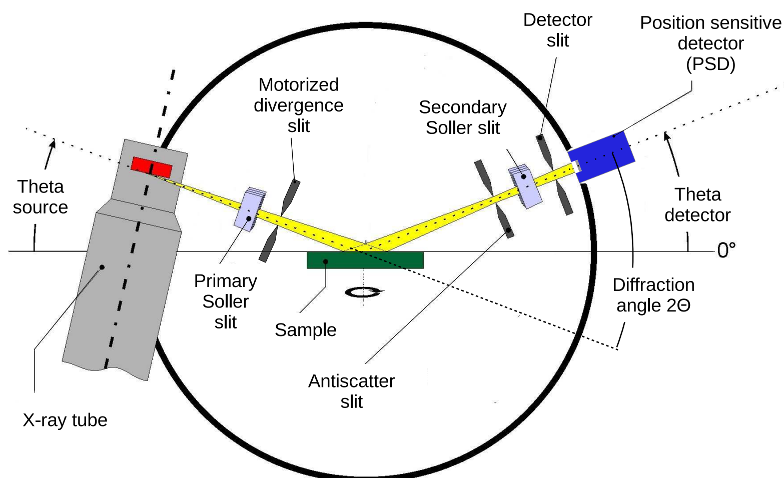

Obrázek 1.2. Bragg–Brentano setup with linear position sensitive detector for powder diffraction measurements.

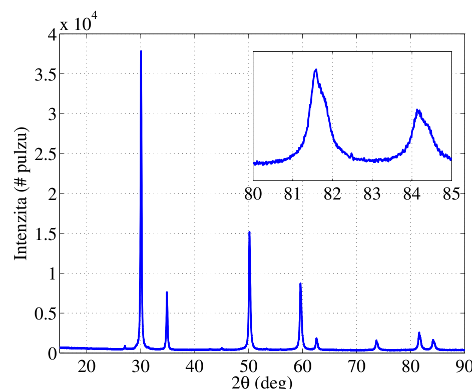

Obrázek 1.3. Example of diffractogramm measured using Bragg–Brentano setup. Inset shows detail of 80–85°.

Fast evaluation can be done using computer programs and database of powder diffraction data (PDB – powder diffraction database, paid license). Free available database is COD (crystallography open database) at webpage: http://www.crystallography.net/cod/

1.5. Width of diffraction peaks

The diffraction line width is given by several factors; the basic ones are the following

- crystallites size
- inhomogeneous strain
- instrumental resolution
- wavelength spread

First we will discuss the crystallites size broadening. The width of the diffraction peak in reciprocal space is inversely proportional to crystallite size, or more precisely size of coherently diffracting domain $\Delta Q \approx \frac{2\pi}{D}$. The scattering vector is proportional to sin of Bragg angle

$$Q = \frac{4\pi}{\lambda} \sin\theta. \tag{1.5}$$

Differentiating preceding formula we obtain formula for angular width of diffraction lines

$$\Delta Q = 2\frac{2\pi}{\lambda} \cos\theta \Delta\theta \approx \frac{2\pi}{D}, \quad \Delta 2\theta \approx \frac{\lambda}{D\cos\theta}. \tag{1.6}$$

More precise derivation of Scherrer formula can be find in literature, see for example [2]

$$2w(2\theta,\text{rad}) = \frac{0.94\lambda}{D\cos\theta}, \tag{1.7}$$

where $2w$ is full width at half maximum of diffraction peak measured in 2θ angle and D is mean crystallite size in the direction perpendicular to diffracting crystallographic planes, i.e. in the direction of the scattering vector. One can express similar formula using integral peak width β, defined as ration of integral peak intensity and its maximum intensity. Then we will obtain Stokes-Wilson formula

$$\beta(2\theta,\text{rad}) = \frac{\lambda}{L\cos\theta}, \tag{1.8}$$

where L is volume averaged crystallite size in the scattering vector direction. The quantities D and L equals for a case of monodisperse particles – all crystallites have the same size. For polydisperse particles those quantities differ according size distribution.

The second contribution to diffraction profile width is an inhomogeneous strain. Let us assume the local inter-planar distance $d + \Delta d$ differs from the average inter-planar distance d by a small difference Δd. The corresponding Bragg angle would by also different by a value $\Delta\theta$ which we can derive differentiating Bragg equation

$$\Delta\theta = -\frac{\Delta d}{d} \tan\theta, \tag{1.9}$$

where $\varepsilon = \frac{\Delta d}{d}$ deformation in the diffraction vector direction. The local deformation has statistical distribution width η and then the diffraction peak would have width

$$\beta(2\theta,\text{rad}) = 4\eta \tan\theta. \tag{1.10}$$

We denote the strain inhomogeneity leads to peak widening; homogeneous strain leads to shift of the diffraction peak.

Total width is convolution of both components. If both profiles are Lorentzian the total width is sum of both components

$$\beta(2\theta,\text{rad}) = \frac{\lambda}{L\cos\theta} + 4\eta \tan\theta. \tag{1.11}$$

Since both contribution has different Bragg angle dependence we can decouple their values. Simple analysis is based on formula multiplied by a factor of $\cos\theta$

$$\beta(2\theta,\mathrm{rad})\cos\theta = \frac{\lambda}{L} + 4\eta\sin\theta, \tag{1.12}$$

which is used to construct Williamson-Hall plot. We plot peak width multiplied by $\cos\theta$ as a function of $\sin\theta$. The graph should show linear dependence whose slope is proportional to strain and absolute value to crystallite size. The Williamson-Hall analysis is very simplified and in present time better methods are used. However, this analysis can still give simple and fast quantitative description of the sample.

The real profiles are widened also by an experimental resolution and non monochromatic radiation. The instrumental resolution is in the first approximation angle independent; the derivation of wavelength spread to a peak width is left to the reader.

Real samples could exhibit very different behavior than previous simplified analysis. Among other effects we would mention crystallite shape and elastic anisotropy. Shape of real crystallites are often elongated in certain crystallographic direction (or could have flat shape). The crystallite size would than strongly vary with scattering vector direction and the peak width would not be monotone function of Bragg angle. Similar effect could have elastic anisotropy; the deformation could vary strongly with crystallographic direction. Those effects could lead to a significant deviation of the formula (1.12).

This analysis is currently not very often used. Nowadays, the most popular methods are fitting of the full diffraction profile and not only width of the peaks is taken into account.

1.6. Experimental setup

The experiment will be performed using X-ray diffractometer Rigaku SmartLab. The components will be x-ray tube with copper anode – voltage 40 kV, current 30 mA, two Soller slits with divergence $\sim 5\,°$, linear position sensitive detector D/Tex Ultra or 2D detector Hypix 3000 .

1.7. Questions

1. Why do we observe line splitting at high diffraction angles (figure 1.3)?

Task 2. Epitaxial thin film diffractometry, reciprocal space mapping

2.1. Deformation and stress in epitaxial layers

In the following text we will suppose cubic material with (001) surface orientation. Cubic materials have three independent elastic parameters C_{11}, C_{12} a C_{44} [4]. Also the substrate is assumed to be much thicker than the layer and therefore not deformed. Lattice parameter of substrate is a_s and lattice parameter of the layer in undeformed state is a_l. The lattice mismatch is defined as

$$\epsilon_l = \frac{a_l - a_s}{a_s}. \tag{2.1}$$

In the general case layer is deformed so its lattice parameters are $a_{\parallel}$ and $a_{\perp}$, in the surface plane and perpendicular to surface, respectively. We can define in-plane deformation $\epsilon_{\parallel}$ and out-of-plane deformation

$$\epsilon_{\parallel} = \frac{a_{\parallel} - a_l}{a_l}, \quad \epsilon_{\perp} = \frac{a_{\perp} - a_l}{a_l}. \tag{2.2}$$

There are possible limiting cases

- Pseudomorph layer – in-plane lattice parameter of layer equals substrate lattice parameter $a_{\parallel} = a_s$; layer is deformed in such a way that it follows substrate. Usually for very thin films or very small mismatch. In-plane deformation equals to negative mismatch value.

$$\epsilon_{\parallel} = -\epsilon_l. \tag{2.3}$$

- Relaxed layer – layer lattice parameters equal the bulk lattice parameter of the layer material $a_{\parallel} = a_{\perp} = a_l$. The layer is not deformed at all; this case occurs for thick films with large lattice mismatch. The deformation is followed with existence of misfit dislocations. Deformation of the layer equals zero

$$\epsilon_{\parallel} = \epsilon_{\perp} = 0. \tag{2.4}$$

- General case – anything between the above mentioned states. We can define degree of relaxation as

$$R = \frac{a_{\parallel} - a_s}{a_l - a_s}, \tag{2.5}$$

  which equals 0 for pseudomorphic layer and 1 for relaxed layer.

- Layer lattice is tilted by an angle ϕ with respect to substrate lattice – figure 2.2 right panel. This case can be combined with the above mentioned cases.

Elastic strain components σ can be evaluated using Hook's law

$$\sigma_{\parallel} = \frac{E}{(1+\nu)(1-2\nu)}\left[\varepsilon_{\parallel} + \nu\varepsilon_{\perp}\right], \quad \sigma_{\perp} = \frac{E}{(1+\nu)(1-2\nu)}\left[(1-\nu)\varepsilon_{\perp} + 2\nu\varepsilon_{\parallel}\right], \tag{2.6}$$

where E is Young's modulus and ν Poisson's ratio. Layer surface is free of force, therefore the out of plane stress equals zero

$$\sigma_{\perp} = 0. \tag{2.7}$$

Using the preceding formula one can obtain the following expression of the stress free layer lattice parameter

$$a_l = \frac{(1-\nu_l)a_{\perp} + 2\nu_l a_{\parallel}}{1+\nu_l}. \tag{2.8}$$

where layer lattice parameter is determined using in-plane $a_{\parallel}$ and out-of-plane lattice parameters $a_{\perp}$ measured using x-ray diffraction. The in-plane stress component than equals

$$\sigma_{\parallel} = \frac{E_l}{1-\nu_l}\epsilon_{\parallel}. \tag{2.9}$$

For cubic lattice and surface orientation (001) following formulas hold for Young's modulus and Poisson's ratio

$$\nu_{001} = \frac{C_{12}}{C_{11}+C_{12}}, \quad E_{001} = \frac{(C_{11}+2C_{12})(C_{11}-C_{12})}{C_{11}+C_{12}}. \tag{2.10}$$

and for (111) orientation

$$\nu_{111} = \frac{1}{2}\frac{C_{11}+2C_{12}-2C_{44}}{C_{11}+2C_{12}+2C_{44}}, \quad E_{111} = 3\frac{(C_{11}+2C_{12})C_{44}}{C_{11}+2C_{12}+C_{44}}. \tag{2.11}$$

2.2. Reciprocal space mapping

This section describes basics of reciprocal space mapping using x-ray diffraction and lattice parameters determination. General experiment scheme is plotted in figure 2.1. Incident beam is described with a wave

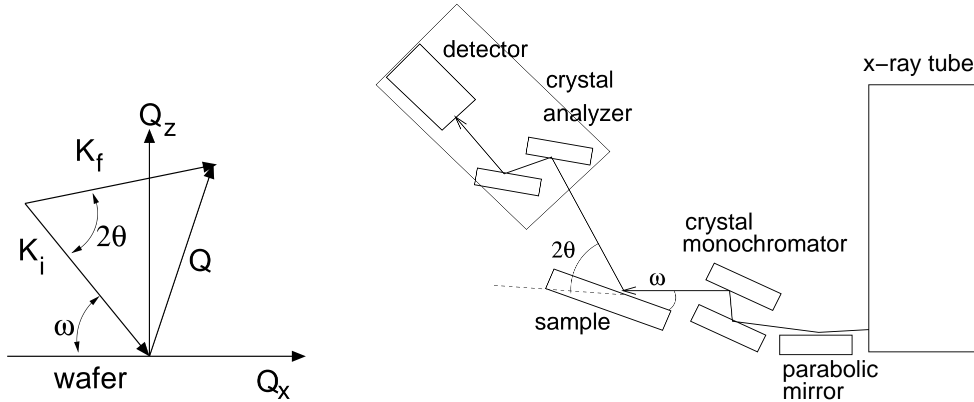

Obrázek 2.1. Left panel: general schematics of x-ray scattering. Right: experimental setup of high-resolution x-ray diffraction with crystal monochromator and analyzer.

vector $\boldsymbol{K}_i$ of a length $K = 2\pi/\lambda$, where λ is wavelength of x-ray radiation. Diffracted beam has wavevector $\boldsymbol{K}_f$ and we define scattering vector $\boldsymbol{Q} = \boldsymbol{K}_f - \boldsymbol{K}_i$. Diffraction maxima are observed if the scattering vector $\boldsymbol{Q}$

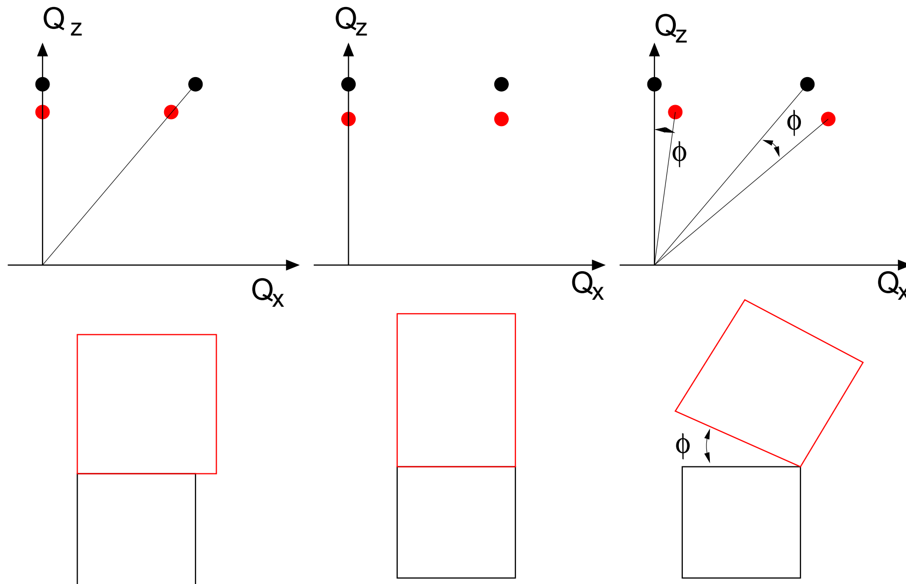

Obrázek 2.2. Top: position of layer (red) and substrate (black) diffraction maxima in a symmetric (points close to Q_z axis) and asymmetric diffraction (right with respect to Q_z axis). Bottom: schematic arrangement of layer and substrate lattices. Left: relaxed epitaxial layer. Center: pseudomorphic epitaxial layer. Right: relaxed and tilted epitaxial layer.

coincides with any reciprocal lattice point. Relative positions of substrate and layer reciprocal lattice points are plotted in figure 2.2 for three examples of relaxed and pseudomorphic layer. In usual definition the axis Q_z denotes surface normal.

At symmetric diffraction the diffraction vector $\boldsymbol{Q}$ is perpendicular to the surface. If the layer lattice is not tilted with respect to the substrate one can easily determine out-of-plane lattice parameter of both substrate and layer

$$Q_{z,l} = \frac{2\pi}{a_\perp} l, \quad \text{and} \quad Q_{z,s} = \frac{2\pi}{a_s} l, \tag{2.12}$$

where l is diffraction order. For tilted lattice the layer diffraction maximum does not lie at Q_z axis; the tilt angle ϕ can be easily determined from the diffraction maximum position according figure 2.2. The in-plane lattice parameter has to be determined using asymmetric diffraction

$$Q_{z,l} = \frac{2\pi}{a_\perp} l, \quad \text{and} \quad Q_{x,l} = \frac{2\pi}{a_\parallel}\sqrt{h^2 + k^2}, \tag{2.13}$$

where these formulas hold for cubic lattice with surface orientation (001) and asymmetric diffraction with Laue indices hkl.

In a case of tilted layer one has to correct the position by a tilt angle ϕ. Therefore both symmetric and asymmetric diffractions are necessary to be measured; tilt angle can be determined using symmetric diffraction and asymmetric one is needed to determine both in-plane and out-of-plane components of lattice parameter. Using known values of Poisson's ratio we can determine the unstrained layer lattice parameter and strain components and relaxation degree using formulas (2.8), (2.2), and (2.5).

2.3. Experimental setup

We will use copper x-ray tube with crystal monochromator and analyzer. The measurement is performed as mapping in two angles ω and 2θ. The experiment is very sensitive to a precise alignment, it is necessary to align properly angle of incidence, tilt angle and azimuthal rotation of the sample.

2.4. Procedure

1. Align sample to measure map of one symmetric and one asymmetric diffractions.
2. Measure intensity distribution in the vicinity of aligned reciprocal lattice points.
3. Determine lattice parameters, tilt angle, strain and relaxation degree of epitaxial layer.

2.5. Questions

1. How to correct diffraction position of tilted layer?

2. How would you align the sample?

Task 3. X-ray reflectivity

3.1. Task formulation

Measurement of x-ray reflectivity on a thin film sample. Determination of layer thickness and roughness of individual interfaces fitting the reflectivity profile.

3.2. Theory

Refraction index od x-ray radiation $n = 1 - \delta + \mathrm{i}\beta$ is very close and smaller than one. According the Fresnel formulae the reflectivity is measurable only for grazing incidence angles. The angle of incidence θ is therefore usually measured with respect to the sample surface in contrary to the common terminology in viible range. Since the material has refraction index smaller than air we can bserve total external reflection at critical angle θ_C (in radians)

$$\theta_C = \arccos n \approx \sqrt{2\delta}. \tag{3.1}$$

Values of δ can be found for example at webpage: http://x-server.gmca.aps.anl.gov/x0h.html [6].

Let us assume sample with thickness t on a substrate, sse figure 3.1. Fresnel coefficients of reflectivity of layer surface and layer-subtsrate interface in a small angle limit can evaluated as

$$\mathfrak{r}_1 = \frac{\theta - \theta_l}{\theta + \theta_l} \quad \text{a} \quad \mathfrak{r}_2 = \frac{\theta_l - \theta_s}{\theta_l + \theta_s}, \tag{3.2}$$

where direction of beam propagation in layer follows Snell's law $\theta_v = \sqrt{\theta^2 - 2\delta_v}$ and in substrate $\theta_s = \sqrt{\theta^2 - 2\delta_s}$.

The amplitude of reflected wave is

$$R(\theta) = \frac{\mathfrak{r}_1 + \mathfrak{r}_2 e^{-\mathrm{i}\phi}}{1 + \mathfrak{r}_1 \mathfrak{r}_2 e^{-\mathrm{i}\phi}}, \tag{3.3}$$

where $\phi = (4\pi/\lambda)\theta_l t$ is a phase retardation of wave in the layer.

Measured intensity $I(\theta)$ is proportional to $|R(\theta)|^2$.

From the previous formulas follows the reflectivity has oscillatory behavior with a pseudo-period of $\theta_l t = t\sqrt{\theta^2 - 2\delta_l}$. The angular position of m-th maximum $\theta^{(m)}$ is then

$$\sqrt{(\theta^{(m)})^2 - \theta_{Cl}^2} = \frac{\lambda}{2t}(m - m_0). \tag{3.4}$$

One can see the maxima are not strictly equidistant, since they are shifted by a angle of total external reflection θ_{Cl}. For the practical evaluation it is easier to introduce the angle of first observable maximum of the order m_0. In many cases the first interference maximum is allways observable. The we can obtain simple linear dependence of the quantity on the left side of formule (3.4) with a slope $\lambda/2t$. In the previous formula we have used small angle limit of gonimetric functions and the angles have to be allways used in radians. The approximate value of interference period for rough thickness determination is $180/\pi \cdot \sqrt{(\lambda/2t)^2 + 2\delta_l}$.

3.3. Experimental setup

X-ray diffractometer equipped with a copper x-ray tube, slits, computer controlled gonimeter and a detector. First the adjustment of the instrument is performed; the zero position of a detector arm angle is adjusted to a direct beam. The next step is sample alignment; sample position and angle of incidence is aligned. The measurement output is a reflectivity curve $I(\theta)$ of a reflected intensity as a function of angle of incidence.

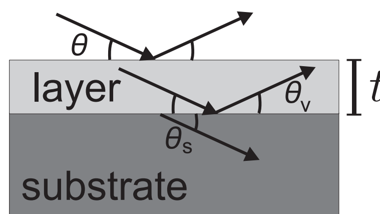

Obrázek 3.1. Schematic drawing of wavevectors in layer/substrate system.

3.4. Data evaluation

Perform simple evaluation of layer thickness using approximative formula (3.4). Also the data will be fitted using specialized software – either the commercial software Rigaku or freeware software GenX [7]. The fitting of full curve will provide us with values of surface and interface roughness and density of individual layers. Compare the obtained resuts with ones obtained using approximative formula.

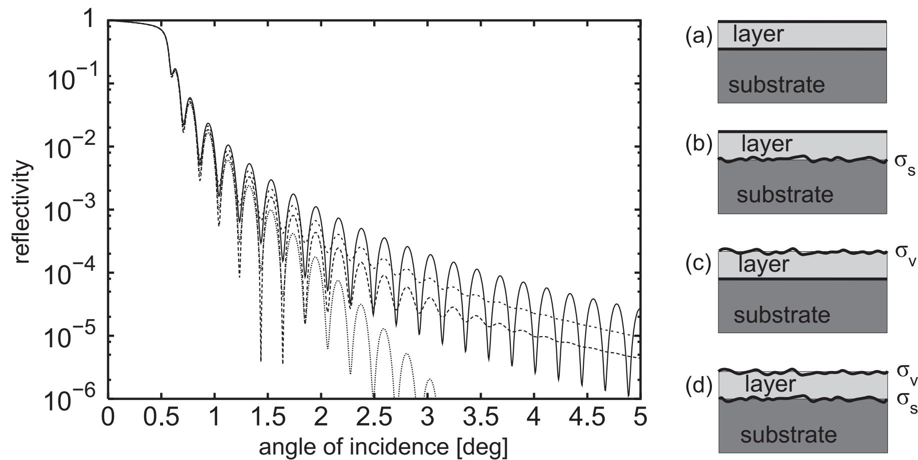

Obrázek 3.2. Reflectivity simulation of 20 nm thick tungsten film on saphire substrate. The interface and surface are smooth or hav roughness of 0.5 nm. Four cases are simulated: (a) both interfaces smooth, (b) surface smooth and interface rough (c) interface smooth and surface rough, and (d) both rough.

3.5. Questions

1. How will affect the measurement finite sizes of the sample and beam at low angles of incidence? Guess the angle when whole beam would irradiate sample surface for realistic parameters (beam size 0.2 mm, sample size 10 mm).

2. How would look reflectivity of semiinfinite sample with an oxide or adsorbed layer at surface? Would affect a single monolayer the experimental data?

3. What is the roughness effect? Try to identify the curves in figure 3.2?

4. The divergence of beam defined using a parabolic mirror is $\sim 0.03°$ and the dynamical range allows us to measure up maximal angle of incidince $\theta_{\max} \sim 5°$. Guess minimal and maximal layer thickness available for x-ray reflectivity experiment.

Task 4. Small angle x-ray scattering

4.1. Task formulation

Measure and analyze small angle scattering of nanoparticles.

4.2. Theory

Small angle scattering is measured at low scattering angle up to 10°. The crystalline ordering usually does not play any role since the lowest diffraction peaks begin to appear at bigger scattering angles. The scattered amplitude is proportional to a Fourier transform of the electron density

$$E(\boldsymbol{Q}) = \int \mathrm{d}\boldsymbol{r} \rho(\boldsymbol{r}) \mathrm{e}^{-\mathrm{i}\boldsymbol{Q}\cdot\boldsymbol{r}}. \tag{4.1}$$

And the scattered intensity is proportional to a square of its absolute value

$$I(\boldsymbol{Q}) = \left| \int \mathrm{d}\boldsymbol{r} \rho(\boldsymbol{r}) \mathrm{e}^{-\mathrm{i}\boldsymbol{Q}\cdot\boldsymbol{r}} \right|^2. \tag{4.2}$$

Assuming constant density of the particles we can express the density distribution using shape function and constant electron density

$$\rho(\boldsymbol{r}) = \rho_0 \Omega(\boldsymbol{r}). \tag{4.3}$$

In many cases the particles are randomly oriented in a dilute solution. As long as the particles are far from each other we can neglect correlation effects of their positions. Then the intensity can be expressed as an orientational average

$$I(Q) = 4\pi \int_0^{D_{\max}} p(r) \frac{\sin Qr}{Qr} \mathrm{d}r, \quad p(r) = \frac{r^2}{2\pi^2} \int_0^\infty Q I(Q) \frac{\sin Qr}{Qr} \mathrm{d}Q, \tag{4.4}$$

where $p(r)$ is distance distribution function.

The distance distribution function of intensity distribution has to be calculated for a given particle shape and size model including size dispersion. We can use several of available software packages. List of them is available online http://smallangle.org/content/software.

4.3. Limiting cases – simple quantitative analysis

Several quantities can be evaluated without fitting, and even without any particle model. At low angle limit the intensity can be expressed using Guinier's formula

$$I(Q) = I_0 \mathrm{e}^{-Q^2 R_g^2/3}, \tag{4.5}$$

where R_g is particle gyration radius. Guinier's plot is logarithm of intensity plotted as a function of square of scattering vector – the intensity dependence in this region is linear. We note the zero angle scattered intensity $I(0)$ cannot be directly measured (because of primary beam) and Giunier fit is one of possibilities to determine its value. Gyration radius is defined using distance distribution function

$$R_g^2 = \frac{\int_0^\infty r^2 p(r) \mathrm{d}r}{\int_0^\infty p(r) \mathrm{d}r}. \tag{4.6}$$

The high angle limit has a power dependence according Porod's law

$$I(Q) = C Q^{-4}, \tag{4.7}$$

where C is a scale parameter. This law is valid for particles with sharp interface. If the particle surface is diffuse or has fractal behavior the exponent changes from 4 to a general exponent $n = 6 - d$, where d fractal dimension of the particle surface. Last of the simple evaluation methods is Porod's invariant

$$P = \int I(Q) Q^2 \mathrm{d}Q \tag{4.8}$$

Combining Porod's invariant P and zero angle scattered intensity $I(0)$ we can get particle volume V_p

$$V_p = \frac{2\pi^2 I(0)}{P}. \tag{4.9}$$

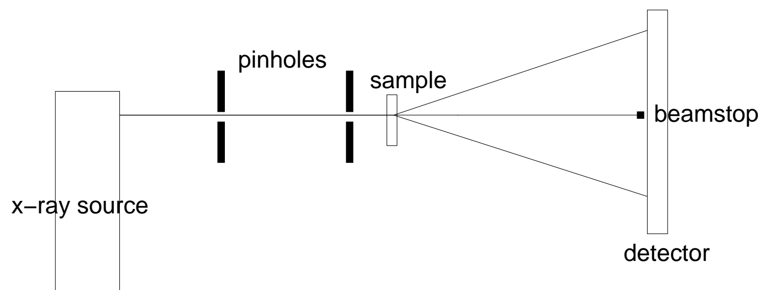

Obrázek 4.1. SAXS setup in transmission geometry with two pinholes.

4.4. Experimental setup

The experiment will be performed in setup with a small beam and two-dimensional detector. The incident beam has to be very narrow and collimated in both directions. The beam will be collimated using two pinholes; one positioned close to the x-ray tube and the other one as close as possible to the sample.

The beam divergence is limited by the pinholes diameter, the smallest ones are 0.1 mm and 0.05 mm. The beam divergence limits the smallest possible scattering vector accessible for experiment. For smaller angles the signal is covered by primary beam. By the properties of Fourier transform it translate to the upper limit of particle size. Typical values are in the order of lowest scattering angle $2\theta \approx 0.1^\circ$, corresponding scattering vector $Q_{\min} \approx 0.007\,\text{Å}^{-1}$ and largest particle size $D = \frac{\pi}{Q_{\min}} \approx 50\,\text{nm}$.

For SAXS in solution the scattered intensity has rotational symmetry. The data of two-dimensional detector will be then azimuthally averaged to increase signal to noise ration and the line profile will be fitted using specialized software.

Literature

[1] U. Pietsch, V. Holý, T. Baumbach, *High-Resolution X-Ray Scattering From Thin Films and Multilayers*, Springer, Berlin, 1999 and 2004.

[2] B. E. Warren, *X-ray diffraction*, Dover Publications, New York 1990.

[3] FullProf homepage: http://www.ill.eu/sites/fullprof/

[4] Lattice parameters of semiconductors: v O. Madelung, *Semiconductors: Data Handbook*, Springer 2004, or http://www.ioffe.ru/SVA/NSM/Semicond/index.html.

[5] Crystallography open database: http://www.crystallography.net/.

[6] Sergey Stepanov's x-ray server: http://x-server.gmca.aps.anl.gov/x0h.html.

[7] Genx homepage: http://genx.sourceforge.net/.